Version of Record: https://www.sciencedirect.com/science/article/pii/S0378381222001947
Manuscript_75399653eb0eab1b3eb08cd14c586b2f

THERMODYNAMIC MODELING OF ADSORPTION AT THE LIQUID-SOLID INTERFACE

Rajasi Shukre[1], Shikha Bhaiya[1], Usman Hamid[1], Hla Tun[1], and Chau-Chyun Chen[1]

[1]*Department of Chemical Engineering, Texas Tech University, Lubbock, Texas 79409, United States*

ABSTRACT

Adsorptive separation techniques are significantly energy efficient in comparison to conventional thermal separation techniques such as distillation. Despite extensive research and development activities undertaken for mixed-gas adsorption, the use of adsorption techniques for the separation of multicomponent liquid mixtures is still limited. A major barrier is the lack of accurate adsorption thermodynamic models, which form the scientific foundation of process simulation of such systems, making the translation to industrial scale challenging. In this work, we have rigorously computed the surface excess of adsorption for six binary liquid mixtures on silica gel at 303 K using the frameworks of the generalized Langmuir isotherm (gL) and the adsorbed solution theory (AST). The six binary liquid mixtures were formed by the pair-wise combinations of four components: benzene, 1,2-dichloroethane, cyclohexane and n-heptane. We have based our calculations by considering simultaneous equilibria of three phases: saturated vapor phase, bulk liquid phase and adsorbed phase. The composition of the corresponding saturated vapor phase was estimated by the Nonrandom Two-Liquid activity coefficient model and experimental vapor-liquid equilibria data. The activity coefficients of the adsorbed phase, the central issue of multicomponent adsorption thermodynamics, were calculated using the adsorption Nonrandom Two-Liquid activity coefficient model. Devoid of simplifying assumptions, gL and AST provide rigorous thermodynamic frameworks for adsorption equilibria of multicomponent liquid mixtures.

1. INTRODUCTION

The selective separation of bulk liquid mixtures has been traditionally performed through distillation [1]. This convention has been highlighted by the fact that there is a vast amount of vapor-liquid equilibria data for a variety of liquid mixtures. Furthermore, the thermodynamics of vapor-liquid equilibria is a well-established field, with a number of activity coefficient models describing the phase behavior of non-ideal mixtures exhibiting large deviations from Raoult's law [2]. Thus, the process simulation, design and optimization of distillation units have been long-standing and ubiquitous practices. However, the primary disadvantage of conventional distillation operation is the cost associated with the reboiler and condenser duty, making this legacy separation process energy-intensive [3].

Adsorption processes have been shown to be highly energy efficient as compared to distillation processes, with higher separation efficiencies even for azeotropic mixtures [4]. Although the simulation and implementation of adsorption processes have been widely studied for the separation of gas mixtures, active research and practice has been missing for the separation of bulk liquid mixtures [5,6]. In the latter case, there is also a scarcity of experimental surface excess data [6]. Therefore, there has not been much work reported on the thermodynamic modeling front for bulk liquid adsorption processes, making the simulation, design and implementation even more challenging.

Some of the early studies on the thermodynamic modeling of adsorption from bulk liquid solutions come from the contributions made by Everett and co-workers, who recognized the correlation between adsorption at the solid-vapor and the solid-solution interface [7]. However, the derived correlations for surface excess were based on several assumptions related to the monolayer structure of the adsorbed phase, nature of the bulk liquid phase and orientation of the adsorbed molecules on the adsorbent surface [7–16], which in turn severely limited the applicability of such models.

The systematic investigation of the thermodynamics of liquid adsorption has been reported by Myers, Sircar and co-workers who developed fundamental expressions for the thermodynamic excess functions associated with liquid adsorption [17]. They measured the surface excess of several liquid mixtures on silica gel, activated carbon, titanium dioxide as

well as graphon and developed a thermodynamic consistency test for the experimental data of surface excess [18,19]. Moreover, they developed a rigorous framework to correlate the adsorption of liquid mixtures to the adsorption of the corresponding vapor mixtures, in the limit of saturation [20]. However, the derivation of the subsequent surface excess expression was based on the assumption of an ideal adsorbed phase [21]. The calculation of the surface excess required sequential solving of multiple equations [22]. Adsorbent heterogeneity was accounted for with a distribution function for site selectivities resulting in a complex expression for the surface excess. [23].

With prior thermodynamic modeling studies of limited applicability, there is a crucial need for rigorous and comprehensive thermodynamic frameworks for liquid adsorption. In this work, we presented two thermodynamic frameworks to estimate the adsorption of binary liquid mixtures using 1) the recently developed generalized Langmuir isotherm (gL) [24] and 2) the classical adsorbed solution theory (AST) including the ideal adsorbed solution theory (IAST) [25] and the related real adsorbed solution theory (RAST) [26-28]. For both frameworks, we have implemented the adsorption Nonrandom Two-Liquid (aNRTL) model for evaluating the adsorbed phase activity coefficients [24, 29], the central issue of multicomponent adsorption thermodynamics. The framework of the gL isotherm is advantageous over the AST framework since gL does not require the computationally expensive calculation of the spreading pressure of the adsorption system, making the gL implementation suitable for process simulation.

We have based our calculations on the equivalence of adsorption from binary liquid mixtures and adsorption from the corresponding saturated binary vapor mixtures, as proposed by Myers and Sircar [20]. The saturation pressure and the composition of the corresponding saturated vapor phase were evaluated using the Nonrandom Two-Liquid (NRTL) activity coefficient model [30]. We have tested the two thermodynamic frameworks for the adsorption of six binary liquid mixtures on silica gel at 303 K: *i*) benzene–1,2-dichloroethane, *ii*) benzene–cyclohexane, *iii*) cyclohexane–1,2-dichloroethane, *iv*) benzene–n-heptane, *v*) cyclohexane–n-heptane, and *vi*) 1,2-dichloroethane–n-heptane [6,18]. These systems were selected because the pure component adsorption isotherm data for each of the four components on silica gel at 303 K was available [6,18].

We have successfully correlated the surface excess for the six binary systems, resulting in a qualitative to semi-quantitative agreement with the experimental surface excess data using the gL framework and a semi-quantitative to quantitative agreement using the AST framework. The thermodynamic frameworks for correlating the adsorption from binary liquid mixtures to the adsorption from the corresponding saturated vapor phase along with discussion of the results are given in the subsequent sections.

2. THERMODYNAMIC FRAMEWORKS

2.1 Thermodynamic System for Liquid Adsorption

The thermodynamic system for the adsorption of binary liquid mixture consists of three phases: the saturated vapor phase, the bulk liquid phase, and the adsorbed phase. The three phases are at equilibrium with one another at a constant temperature T, as shown in Figure 1 [18]. The bulk liquid phase consists of liquid components 1 and 2. Upon contacting the binary liquid mixture with a solid adsorbent, adsorption of the two components occurs to form the adsorbed phase. After establishment of equilibrium between the two phases, the mole fractions of components 1 and 2 in the bulk liquid phase are denoted as x_1 and x_2, respectively, whereas the mole fractions of the two components in the adsorbed phase are denoted as x_1' and x_2', respectively. Moreover, the bulk liquid phase is also in equilibrium with its saturated vapor phase at the given temperature, with the vapor phase mole fractions denoted as y_1 and y_2 for the components 1 and 2, respectively.

Therefore, equilibrium conditions are established among the saturated vapor phase, the bulk liquid phase, and the adsorbed phase. This can be expressed in terms of the equivalence of fugacity of each component in the three phases, which is given below in equation 1.

$$f_i^{vap}\,(T, P^s, y_i) = f_i^{liq}\,(T, P^s, x_i) = f_i^{ads}\,(T, P^s, x_i') \tag{1}$$

Here, f_i^{vap}, f_i^{liq} and f_i^{ads} are the fugacities of the component i in the vapor, liquid, and adsorbed phase, respectively. The equilibrium conditions for the vapor-liquid equilibrium and

the adsorption equilibrium are the system temperature T and the saturation pressure P^s, which is the liquid mixture bubble point pressure at the system temperature T.

At equilibrium, the surface excess of component 1 in the adsorbed phase, n_1^e is given by equation 2 [31]

$$n_1^e = n'(x_1' - x_1) \tag{2}$$

Here, n' is the total number of moles adsorbed onto the adsorbent surface, x_1' and x_1 are the equilibrium mole fraction of component 1 in the adsorbed phase and the bulk liquid phase, respectively. The surface excess of each component can be determined experimentally by measuring the mole fraction of each component in the bulk liquid phase, before and after adsorption [31].

Based on the aforementioned equilibrium between the three phases, it has been shown previously [20] that the surface excess of components 1 can also be obtained from the experimental data of adsorption of the unsaturated vapor mixture of components 1 and 2, by the following relation given in equation 3.

$$n_1^e = \lim_{P \to P^s} n'(x_1' - x_1) \tag{3}$$

Thus, the adsorption of the binary liquid mixture can also be considered as the adsorption of the corresponding vapor mixture, in the limit of the pressure approaching the saturation pressure P^s of the liquid mixture at the given temperature. The two thermodynamic frameworks used in this work to estimate the surface excess of binary liquid adsorption are described in the next sections.

2.2 Generalized Langmuir isotherm

The first thermodynamic framework considered in this study for the calculation of liquid adsorption as the adsorption of the corresponding vapor mixture is the generalized Langmuir isotherm (gL) [24]. gL is an extension and generalization of the thermodynamic Langmuir isotherm (tL) for pure component adsorption [32-34]. tL accounts for the adsorbent heterogeneity by expressing the adsorption-desorption equilibria in terms of the activities of the adsorbate and the vacant sites modeled as the phantom molecule ϕ, as opposed to the

concentrations of the same used in the classical Langmuir isotherm [35]. The adsorbed phase activity coefficients were calculated using the aNRTL model [24,29]. Subsequently, gL extends this concept for competitive multicomponent adsorption and further generalizes it by taking into account the variation of saturation loadings of pure adsorbates due to adsorbate molecule size differences. This physical reality is addressed in gL by considering a constant total surface area of the adsorbent, which can be expressed in terms of the product of saturation loading and cross-sectional area of adsorbate molecule. In addition, the aNRTL model in tL is replaced by an area-based aNRTL model in gL [24]. As a generalization of tL, gL is applicable for both pure component and mixed-gas adsorption equilibria.

The surface area of adsorption for a given adsorbent is usually reported in the literature. The cross-sectional area of the adsorbate molecule on the adsorbent at the given temperature is also available from the literature. The phantom molecule is chosen to be the nitrogen molecule. Thus, the total area of the adsorbent is given as follows,

$$A^o = n_i''^0 A_i = n_\phi''^0 A_\phi \tag{4}$$

Where, A^o is the surface area of the adsorbent, superscript "''" refers to the adsorbed phase with the vacant sites considered as "occupied" by the phantom molecule ϕ; $n_i''^0$ and $n_\phi''^0$ are the saturation loadings of the adsorbate component i and the phantom molecule ϕ, respectively; A_i and A_ϕ are the corresponding molecular cross-sectional areas.

Thus, for pure component or mixed-gas adsorption consisting of m adsorbate components, the area fractions of the adsorbate component i and the phantom molecule ϕ can be computed by the following equations,

$$\theta_i'' = \frac{n_i'' A_i}{A^o} = \frac{n_i''}{n_i''^0} = \frac{K_i^o y_i P}{\frac{\gamma_i''}{\gamma_\phi'' q_i} + \sum_{j=1}^{m} \frac{\gamma_i'' q_j}{\gamma_j'' q_i} K_j^o y_j P} \tag{5}$$

$$\theta_\phi'' = \frac{n_\phi'' A_\phi}{A^o} = \frac{n_\phi''}{n_\phi''^0} = \frac{1}{1 + \sum_{j=1}^{m} \frac{\gamma_\phi'' q_j}{\gamma_j''} K_j^o y_j P} \tag{6}$$

Where, $q_i = \frac{A_i}{A_\phi}$, and θ_i'' and θ_ϕ'' are the area fractions of the adsorbate component i and the phantom molecule ϕ, respectively; n_i'' and n_ϕ'' are the corresponding amounts adsorbed; γ_i'' and γ_ϕ'', are the adsorbed phase activity coefficients; K_i^o is the adsorption equilibrium constant; y_i is the mole fraction in the bulk vapor phase with the total pressure P in the vapor phase. In the case of binary liquid adsorption, P is replaced by P^s, the bubble point pressure of the liquid mixture at the system temperature T.

Thus, according to equations 5 and 6, mixed-gas adsorption containing m adsorbate components is treated as a system of $m+1$ components. In other words, pure component adsorption is treated as a binary system consisting of the adsorbate molecule and the phantom molecule. Similarly, binary gas adsorption is treated as a ternary system consisting of two adsorbate molecules and the phantom molecule.

The activity coefficients used in equations 5 and 6 are computed by an area-based aNRTL model, which takes into account adsorbate-adsorbent interactions and sizes of adsorbate molecules [24]. The activity coefficient equation of the aNRTL model is given in equation 7.

$$ln\gamma_i'' = q_i \sum_{j=1}^{m} \frac{x_j''^2 q_j^2 \tau_{ij}'' [G_{ij}'' - 1]}{\left[\sum_{k=1}^{m} x_k'' q_k G_{kj}''\right]^2} \tag{7}$$

Where, $\tau_{ij}'' = -\tau_{ji}''$, $\tau_{ii}'' = \tau_{jj}'' = 0$, $G_{ij}'' = \exp(-\alpha\tau_{ij}'')$, γ_i'' is the adsorbed phase activity coefficient. τ_{ij}'' is the binary interaction parameter and α is the non-randomness factor, set to the value of 0.3 per the convention of the NRTL model [30]. The reference state for the adsorbed phase activity coefficient is the pure adsorbate at saturation loading at the system temperature [24]. Named the "true" mole fractions in the adsorbed phase, x_j'' and x_k'' include the contribution of the vacant sites counted as phantom molecules. For the case of binary vapor adsorption, there will be activity coefficients, γ_1'', γ_2'' and γ_ϕ'', for the two adsorbate components 1, 2 and the phantom molecule ϕ.

In order to compare the calculated mole fractions with the experimental mole fractions, the "apparent" mole fractions, x_1' and x_2', are calculated as given below.

$$x_1' = \frac{x_1''}{x_1'' + x_2''} \quad , \quad x_2' = \frac{x_2''}{x_1'' + x_2''} \tag{8}$$

Thus, in the case of binary liquid adsorption, the expression for the surface excess using gL is given below and has the same mathematical form as equation 2.

$$n_1^e = n'(x_1' - x_1) \tag{9}$$

In equation 9, $n' = n_1'' + n_2''$. For the case of pure component adsorption, given the values of A^o and A_i in the literature, gL requires only two adjustable parameters, K_i^o and $\tau_{i\phi}''$. Hence, using the evaluated pure component isotherm parameters, the mixed-gas adsorption using gL requires only one adjustable parameter, τ_{12}''. The regression of the τ_{12}'' parameter for the adsorption of saturated binary vapor mixture corresponding to the binary liquid mixture is performed by minimizing the objective function, which is the maximum likelihood objective function [36] shown in equation 10.

$$Obj = \sum_l \left(\frac{n_{1,calc,l}^e - n_{1,exp,l}^e}{\sigma_{exp}} \right)^2 \tag{10}$$

Here, $n_{1,calc}^e$ and $n_{1,exp}^e$ refer to the calculated and experimental surface excess amounts of component 1 while σ_{exp} is the standard deviation in the measurement of surface excess and is set to 0.05 *mol/kg*; l is the index for the experimental data points.

The computational load for the gL isotherm is very low, in contrast to the AST framework, where most of the computational time is spent on satisfying the spreading pressure constraint. Furthermore, gL has been shown to significantly improve the correlations of IAST, RAST and extended Langmuir for mixed-gas adsorption [24]. The detailed algorithm for the implementation of the gL isotherm applied to the adsorption of the binary liquid mixture is shown in Figure 2.

2.3 Adsorbed solution theory

The second thermodynamic framework considered in this study for the calculation of liquid adsorption as the adsorption of the corresponding vapor mixture is the adsorbed solution theory. According to the ideal adsorbed solution theory and the related real adsorbed

solution theory, [25,26–28] the equilibrium between the vapor phase and the adsorbed phase can be described by a modified Raoult's law type expression given by equation 11.

$$P^s y_i = P_i^o(T,\pi) x_i' \gamma_i'(T,\pi,x_i') \tag{11}$$

Here, P_i^o is the vapor pressure of pure adsorbate component i at the system temperature T and the spreading pressure π [25]; γ_i' is the adsorbed phase activity coefficient. The difference between IAST and RAST is that the activity coefficients are ignored or set to unity with IAST and accounted for with RAST. The meaning of all other variables has been described in the previous sections. Thus, equation 11 can be used to calculate the apparent mole fraction of component 1, x_1', which is needed for the surface excess calculation in equation 2. The value of the total amount adsorbed, n', is also required in the surface excess calculation. This value can be calculated using an expression from IAST [25], given in equation 12.

$$\frac{1}{n'} = \frac{x_1'}{n_1'(P_1^o)} + \frac{x_2'}{n_2'(P_2^o)} \tag{12}$$

Here, $n_i'(P_i^o)$ is the amount adsorbed for pure component i at the system temperature T and pure adsorbate vapor pressure P_i^o. This expression has been derived by an expression for the change in the area due to mixing, Δa^m, at constant T and π [25], given by equation 13

$$\begin{aligned} \Delta a^m(T,\pi,x_i') &= a(T,\pi,x_i') - \sum_{i=1}^{2} x_i'\, a_i^0(T,\pi) \\ \Delta a^m(T,\pi,x_i') &= RT \sum_{i=1}^{2} x_i' \frac{\partial ln\gamma_i'}{\partial \pi} \end{aligned} \tag{13}$$

Here, a represents the area of the adsorbent per mole of the total adsorbate amount adsorbed, and a_i^0 is the area of the adsorbent per mole of the pure adsorbate adsorbed at the system T and π. For an ideal adsorbed phase, the activity coefficient of each component is unity and therefore, the area change upon mixing at constant T and π is zero. Thus, equation 12 can be derived using equation 13 for an ideal adsorbed phase. For a real adsorbed phase, the area change upon mixing may not be zero. However, in the special case of adsorption from the

liquid phase, or the corresponding adsorption from its saturated vapor phase, the surface coverage is high (*see* § *3.2* for a detailed discussion). Therefore, at high loading which in the current case corresponds to the relative pressure of unity, the activity coefficient will be a weak function of the spreading pressure [37]. Thus, the change in the area due to mixing should be negligible and equation 12 should still be applied to a real adsorbed phase.

The utility of equations 11 and 12 depends on the computation of the other variables involved in the equations. The vapor phase compositions y_i and the saturation pressure P^s corresponding to the given liquid phase compositions x_i and the system temperature T were calculated using experimental vapor-liquid equilibrium data. These calculations were performed by regressing the parameters of the NRTL model [30] in Aspen Properties® V11 (*described in the* § *2.4*).

In this work, the pure component gL isotherm [24] (*see* § *2.2*) was used to calculate the equilibrium amount adsorbed as a function of pressure for each pure adsorbate component constituting the binary mixture, using the available experimental data for pure vapor adsorption [6,18]. The spreading pressure of each pure component was subsequently computed as a function of vapor phase pressure using the Gibbs adsorption isotherm equation [25] given below.

$$\frac{d\pi_i}{dlnP} = \frac{n_i' RT}{A^o} \tag{14}$$

Here, n_i' is the equilibrium amount adsorbed for the pure component i at the pressure P. For the case of binary vapor adsorption equilibrium, the spreading pressure of each adsorbate component must equal to the mixture spreading pressure [25],

$$\pi_1 = \pi_2 = \pi_{mixture} \tag{15}$$

Thus, the spreading pressure of the mixture was computed to satisfy the relation of equation 15. The mixture spreading pressure was required to compute the values of P_i^o and $n_i'(P_i^o)$. The activity coefficient of each component in the adsorbed phase was calculated using the aNRTL model [29]. This thermodynamically consistent activity coefficient model has been successful in representing non-ideal behavior of binary gas adsorption as functions of the

adsorbed phase mole fractions and temperature for different adsorbents [29,33]. The expressions for the activity coefficient of each component were derived [29] and are given by equation 16.

$$ln\gamma_1' = \frac{x_2'^2\tau_{12}'[G_{12}'-1]}{[x_1'G_{12}'+x_2']^2},\ ln\gamma_2' = \frac{x_1'^2\tau_{21}'[G_{21}'-1]}{[x_2'G_{21}'+x_1']^2} \quad (16)$$

Here, $\tau_{12}' = -\tau_{21}'$ and $G_{12}' = \exp(-\alpha\tau_{12}')$, τ_{12}' is the binary interaction parameter. The reference state for the aNRTL model is the pure adsorbate at the system temperature and the spreading pressure of the mixture [29]. The binary interaction parameter was regressed using the experimental data for the surface excess with the objective function given in equation 10. The detailed algorithm for the application of the Adsorbed Solution Theory to model the equilibrium adsorption for a binary liquid mixture is shown in Figure 3. The same algorithm was also used to predict the surface excess using IAST, by fixing the τ_{12}' parameter to 0.

2.4 Vapor-liquid Equilibria (VLE)

The vapor phase composition corresponding to each binary liquid mixture was estimated using the NRTL activity coefficient model [30] in Aspen Properties® V11. The experimental data used in the regression of the binary interaction parameter of the NRTL model was retrieved from the

Aspen Properties® V11 database. The experimental data consisted of isothermal PXY data (293-360 K) and isobaric TXY data (0.39 - 1 bar). The details of the experimental data used in this work are provided in the Tables S1-S7 of the Supplementary Information. The regressed NRTL binary interaction parameters were used in the bubble point flash calculations at 303 K to generate the vapor phase composition and saturation pressure corresponding to the given liquid phase composition for each binary system. Thus, this set of data was subsequently used as an input to the code, which computed the surface excess of each binary system using the gL and AST frameworks.

3. RESULTS AND DISCUSSION

3.1 Estimations of vapor phase composition and saturation pressure

The six binary liquid mixtures studied in this work are: *i*) benzene (1)−1,2-dichloroethane (2), *ii*) benzene (1)−cyclohexane (2), *iii*) cyclohexane (1)−1,2-dichloroethane (2), *iv*) benzene (1)−n-heptane (2), *v*) cyclohexane (1)−n-heptane (2), and *vi*) 1,2-dichloroethane (1)−n-heptane (2). The experimental data of the surface excess of the six binary liquid mixtures adsorbed on silica gel at 303 K was taken from the previous studies [6,18].

The details of the regressed binary interaction parameters of the NRTL model are shown in Tables S8-S9. The comparison of the NRTL model correlations of the PXY data to the experimental data of the same at different temperatures for each binary system is shown in Figure S1. It can be seen from Figure S1 that the correlation of isothermal VLE data at different temperatures agrees well with the corresponding experimental data for all the systems. Moreover, the Root-Mean-Square-Error of the regression is very low for all the systems (See Table S8). Therefore, it can be concluded that the NRTL activity coefficient model is suitable for the calculation of the vapor phase composition and saturation pressure for each binary liquid mixture at 303 K.

3.2 Correlations of pure component isotherms

Table 1: **Pure component gL parameters for adsorption on silica gel at 303 K.** *P_i^s is the saturation pressure of the pure adsorbate, A^o is the surface area of adsorbent reported in the literature [18], $n_i''^0$ is regressed from the experimental isotherms and $A_i = A^o / n_i''^0$; The area of n-heptane has been adjusted by 20% from the original case [38] and the two gL parameters are regressed (n-heptane(adj.)).*

Adsorbates	P_i^s (*bar*)	A_i (*nm²/molecule*)	A^o (*m²/g*)	$n_i''^0$ (*mol/kg*)	K_i^o (*bar⁻¹*)	$\tau''_{i\phi}$	RMSE (*mol/kg*)	ARD (%)	Ref. (Exp.)
1,2-dichloroethane	0.13	0.248	660	4.42±0.04	111.97±3.21	-1.73±0.07	0.17	8.00	[18]
benzene	0.16	0.251	660	4.35±0.02	73.24±1.60	-1.42±0.03	0.10	5.37	[6]
cyclohexane	0.16	0.296	660	3.7±0.02	26.00±0.26	0±0.06	0.13	9.25	[6]
n-heptane	0.075	0.430	660	2.55±0.05	102.25±4.26	-0.55±0.34	0.06	9.83	[6]
n-heptane (adj.)	0.075	0.350	660	3.13	55.19±0.53	-1.52±0.02	0.15	8.70	[6]

The pure component gL parameters of the four adsorbates (1,2-dichloroethane, benzene, cyclohexane, n-heptane) adsorbed on silica gel at 303 K were regressed using experimental pure vapor isotherms [6,18]. These parameters were needed in the input of the gL

calculations for binary liquid adsorption as shown in Figure 2. These parameters were also required to compute the spreading pressure of each component as a function of the pressure *(see equation 14)* in the AST framework. The pure component isotherm parameters are tabulated in Table 1. The plot of pure component spreading pressure as a function of the pressure is given in Figure S2A.

Given in Figure S2B, the plot of the vacant site area fraction as a function of the relative pressure is calculated using the gL isotherm for the pure component adsorption. It shows that more than 80% of the surface area is covered by the pure adsorbate molecules at the relative pressure of unity. Since pure vapor adsorption at the relative pressure of unity is the limiting case of binary liquid adsorption, we can conclude that the surface coverage is high for the case of binary liquid adsorption, and the adsorbed phase activity coefficients (γ_i') are weakly dependent on the spreading pressure and approach a constant value [37], validating the use of equation 12 for RAST.

The surface area of silica gel, A^o, which was used for the measurements of the pure vapor isotherms of the four adsorbates and the subsequent surface excess of the corresponding binary liquid mixtures was reported to be 660 m^2/g in the literature [18]. The molecular cross-sectional area of each of the four adsorbates, A_i, was calculated using equation 4 by regressing the saturation loading, $n_i''^0$, of each pure adsorbate on silica gel, using experimental pure vapor isotherm data [6,18].

There were three methods reported in the literature [39] for the calculation of the molecular cross-sectional area of the adsorbate molecules. The first method involved using the two-dimensional (2D) Van der Waals constant, b^0, calculated using the critical properties of the component [40]. However, this method was based on the assumption of the applicability of the Van der Waals equation of state to the vapor phase and the adsorbed phase [40]. The second method used liquid density values of the components at 303 K and the assumption of spherical molecules, with hexagonal packing [39]. Hence, the first two methods were not very robust due to the simplifying assumptions involved in the calculation of A_i. The third method used the adsorption measurements from different sources to calculate the molecular cross-sectional area of the four adsorbates [39]. However, this method lacked consistency as silica gel is an amorphous adsorbent and therefore, the structure of the porous

network would vary with the synthesis process and the manufacturer. Thus, different sources reported drastically different A_i values for the same adsorbate-adsorbent system at any given temperature [39].

In this work, a comparison and analysis of the gL representation of the pure vapor isotherms was performed for all the three methods of computing the molecular cross-sectional area of the adsorbates. This is shown in Figure S3 and Table S10. It can be seen in Table S10 that the average relative deviation (ARD) (see equation 17) of the pure gL correlations at 303 K involving the calculation of A_i using the first two methods (Van der Waals constant and liquid density) was more than 10% for all the four adsorbates. Moreover, the pure gL correlations with A_i calculated using the third method (adsorption experiments) and reported in the literature [39] resulted in ARD > 15% for all the four adsorbates. Thus, in this work, the regression of $n_i''^0$ and hence the calculation of the molecular cross-sectional area of the adsorbates, A_i, was deemed necessary. Thus, three pure gL parameters, $n_i''^0$, K_i^o and $\tau_{i\phi}''$, were regressed in this work from the experimental pure vapor isotherms for each of the four adsorbates [6,18].

Table 2: **Binary interaction parameters of the IAST, RAST and gL correlations for adsorption of binary liquid mixtures on silica gel at 303 K**. *Here the molecular cross-sectional area of n-heptane is 0.43 nm^2/molecule calculated using regressed $n_i''^0$ from the pure vapor isotherms.*

		gL		IAST			RAST		
System	τ_{12}''	**ARD (%)**	**RMSE**	τ_{12}'	**ARD (%)**	**RMSE**	τ_{12}'	**ARD (%)**	**RMSE**
benzene (1) – 1,2-dichloroethane (2) [18]	0.26± 0.13	26.07	0.020	0	61.90	0.05	0.40±0.13	57.45	0.05
benzene (1) – cyclohexane (2) [6]	0±0.06	37.50	0.41	0	14.42	0.12	-0.90±0.04	17.41	0.15
cyclohexane (1) – 1,2-dichloroethane (2) [18]	-0.01±0.06	43.32	0.23	0	29.17	0.07	1.38±0.26	27.25	0.03
benzene (1) – n-heptane (2) [6]	-1.05±0.03	93.44	0.92	0	16.30	0.11	-1.20±0.09	16.10	0.16
cyclohexane (1) – n-heptane (2) [6]	-0.58±0.07	–	0.03	0	–	0.007	-0.24±0.37	–	0.007
1,2-dichloroethane (1) – n-heptane (2) [18]	0±0.03	99.80	0.99	0	25.43	0.18	0±0.02	21.37	0.13

Figure 4 shows that the representation of the pure component isotherms using gL is in line with the experimental data [6,18] for all the systems, with the average relative deviation (ARD) ≤ 10% in all the four cases (see Table 1). Moreover, the area of n-heptane has been adjusted by 20% from 0.43 $nm^2/molecule$ to 0.35 $nm^2/molecule$ to examine the effect of the cross-sectional molecular area value on the binary surface excess correlations, which is explained in the next subsection. The value of 20% is based on a recent systematic investigation by Cai et al. [38] who suggested the uncertainties associated with experimental data of pure and binary mixture loadings to be ±20%. The corresponding pure gL parameters for n-heptane are tabulated in Table 1, with the ARD further reduced to 8.70% as opposed to 9.83% in the original case. The representation of this case is shown by the dashed line in Figure 4.

3.3 Correlations of Surface Excess – gL and AST Results

The aNRTL binary interaction parameters of the gL isotherm framework and the IAST and RAST frameworks, the two AST variants, for the adsorption of the six binary liquid mixtures on silica gel at 303 K are shown in Table 2. It also contains information on the average relative deviation (ARD) and the root-mean-square-error (RMSE) of the regression, both calculated for N experimental data points, which are defined as follows,

$$ARD\ (\%) = \frac{100}{N}\sum_{l=1}^{N}\left|\frac{n^e_{1,calc,l} - n^e_{1,exp,l}}{n^e_{1,exp,l}}\right| \tag{17}$$

$$RMSE = \sqrt{\frac{\sum_{l=1}^{N}\left(n^e_{1,calc,l} - n^e_{1,exp,l}\right)^2}{N}} \tag{18}$$

The experimental data [18] and the correlation results for the surface excess of the binary system of benzene (1)−1,2-dichloroethane (2) on silica gel at 303 K are shown in Figure 5. It can be seen from Figure 5 that 1,2-dichloroethane is the preferentially adsorbed component on silica gel at 303 K. Therefore, the surface excess of benzene is negative. This trend in the surface excess is captured by the gL and AST frameworks. In fact, the pure component

isotherms and the spreading pressure plot shown in Figure 4 and Figure S2, respectively, indicate that 1,2-dichloroethane is slightly more adsorbed on silica gel at 303 K than benzene for the entire relative pressure range from 0 to 1. Thus, the absolute value of the surface excess is small, and this is also captured. The aNRTL binary interaction parameters of gL and RAST are 0.26 and 0.40 (see Table 2), indicative of small deviations from ideality. The gL correlation agrees quantitatively with the experimental data for this system [18,21] with ARD of 26%. Overestimating the surface excess throughout the entire liquid phase composition, both IAST and RAST qualitatively represented the data with ARD of 62% and 57%, respectively.

Table 3: **Binary interaction parameters of the gL framework for adsorption on silica gel at 303 K of three binary liquid mixtures, each with n-heptane as one component**. *Here the molecular cross-sectional area of n-heptane has been adjusted to 0.35 nm^2/molecule [38] (See Table 1 for pure gL parameters).*

	gL *(n-heptane(adj.))*		
System	τ''_{12}	**ARD (%)**	**RMSE**
benzene (1)–n-heptane (2) [6]	-0.02±0.07	45.93	0.52
cyclohexane (1)–n-heptane (2) [6]	-0.11±0.40	–	0.03
1,2-dichloroethane (1)–n-heptane (2) [18]	0.004±0.02	61.09	0.57

The surface excess correlations of benzene (1)–cyclohexane (2) on silica gel at 303 K by the frameworks are compared with the experimental data [6] of the same as shown in Figure 6. In this case, the surface excess of benzene is positive, indicating that benzene is the preferred component over cyclohexane. The same can be inferred from the pure component adsorption isotherms of Figure 4 and the spreading pressure plot of Figure S2. With Figure 4 showing benzene significantly more adsorbed on silica gel at 303 K than cyclohexane for the entire relative pressure range, the absolute value of the surface excess is much larger than that of the binary system of benzene (1)–1,2-dichloroethane (2). The ARDs of the gL, IAST, and RAST correlations are 37%, 14%, and 17%, respectively. In short, gL qualitatively while

IAST and RAST quantitatively represented the surface excess of benzene (1)−cyclohexane (2) binary system on silica gel at 303 K.

The experimental data [18] and the correlations of surface excess of cyclohexane (1)−1,2-dichloroethane (2) on silica gel at 303 K are shown in Figure 7. The adsorption isotherms of Figure 4 indicate 1,2-dichloroethane to be more favorably adsorbed on silica gel at 303 K than cyclohexane for all values of relative pressure. Hence the surface excess of cyclohexane is negative, as can be seen from the experimental data [18] and the correlations in Figure 7. This can be explained on the basis of the adsorption of the previous two binary systems on silica gel at 303 K: benzene (1)−1,2-dichloroethane (2) and benzene (1)−cyclohexane (2). Since 1,2-dichloroethane is the preferred component over benzene (See Figure 5) and benzene is the preferred component over cyclohexane (see Figure 6), it makes sense that 1,2-dichloroethane would be the preferred component over cyclohexane (see Figure 7). The correlations of surface excess all agree semi-quantitatively with the experimental data [18], with ARD of 43%, 29%, and 27% for gL, IAST and RAST respectively.

The experimental surface excess data of benzene (1)−n-heptane (2) [6] along with the three correlations are shown in Figure 8. It can be seen that the trend of the positive surface excess of benzene in the experimental data is in line with the pure component isotherms of Figure 4 and spreading pressure plot of Figure S2. With ARD of 16%, both the IAST and RAST correlations agree quantitatively with the experimental surface excess data,

The gL correlation, with n-heptane molecular area calculated using regressed n_i'', suggests azeotropic behavior at x_1= 0.58. This is against the experimental surface excess data, where the silica gel preferentially adsorbs benzene for the entire range of bulk liquid compositions [6]. This was resolved by adjusting the area of n-heptane from 0.43 $nm^2/molecule$ to 0.35 $nm^2/molecule$, keeping the area of the adsorbent fixed at 660 m^2/g. Thus, with the adjusted pure gL parameters of n-heptane (see Table 1), gL correlated the experimental surface excess data qualitatively with ARD reduced from 93% in the previous case to 45% (see Table 3). This finding emphasizes the importance of the availability of accurate experimental data of the pure component isotherms required for the regression of pure gL parameters. Moreover, this result signifies that, with the ±20% uncertainties associated with experimental adsorption data of pure components and binary mixtures [38], the pure gL parameters should preferably

be regressed by reconciling the pure and binary adsorption data simultaneously. It should be noted that the adjusted molecular cross-sectional area of n-heptane does not significantly change the IAST and RAST correlations for the adsorption of binary liquid mixture of benzene (1)−n-heptane (2) on silica gel at 303 K.

The surface excess of the cyclohexane (1)−n-heptane (2) mixture on silica gel at 303 K is shown in Figure 9. The experimental surface excess is negligible in this case [6]. This has been rationalized in a previous study [18] by the cross-over of the pure component isotherms of cyclohexane and n-heptane. Moreover, the spreading pressure plot of Figure S2 indicates the equality of the spreading pressure of the two pure components at a relative pressure of 1. This may result in the silica gel having no particular preference for either of the two components. This is also represented by the IAST and RAST correlations, in line with the previous work [21].

gL calculated a slight negative surface excess for cyclohexane. However, the gL correlation with the adjusted area of n-heptane resulted in negligible surface excess, thus representing the experimental data quite well (See Table 3). It once again highlights the significance of having accurate molecular area values of the adsorbates by reconciling both the pure and binary adsorption data. Similar to the previous case, the adjusted molecular cross-sectional area of n-heptane does not significantly change the IAST and RAST correlation results.

The experimental surface excess of 1,2-dichloroethane (1)−n-heptane (2) on silica gel at 303 K [18] with the correlation results are shown in Figure 10. The surface excess is positive for 1,2-dichloroethane for the entire range of liquid composition. Both the IAST and RAST correlations agree well with the experimental data, with ARD of 25% and 21% for the IAST and RAST correlations respectively.

gL suggests an azeotrope in the surface excess at x_1= 0.78. However, the gL correlation with the adjusted n-heptane molecular area of 0.35 $nm^2/molecule$ depicts a qualitative agreement with the experimental surface excess for a major part of the liquid mixture composition. It shows a small preference for n-heptane from x_1 = 0.94 onwards. The ARD was significantly reduced to 61% (See Table 3) after adjusting the n-heptane molecular area by 20%. Again, the results of the IAST and RAST correlations were not affected significantly with the adjusted molecular area of n-heptane.

Interestingly, with the adjusted molecular area of n-heptane, the binary interaction parameters of gL correlations are nearly zero for adsorption of the six binary liquid mixtures on silica gel at 303 K (See Tables 2 and 3). This observation is consistent with the satisfactory IAST correlations for the six systems. In other words, both gL and IAST suggest ideal adsorbed phase behavior for the six systems examined in this study.

4. CONCLUSIONS

This work presents a comprehensive thermodynamic modeling approach for the adsorption of six binary liquid mixtures on silica gel at 303 K. The six liquid mixtures are: *i*) benzene (1)−1,2-dichloroethane (2), *ii*) benzene (1)−cyclohexane (2), *iii*) cyclohexane (1)−1,2-dichloroethane (2), *iv*) benzene (1)−n-heptane (2), *v*) cyclohexane (1)−n-heptane (2), and *vi*) 1,2-dichloroethane (1)−n-heptane (2).

We have considered the adsorption from a binary liquid mixture to be equivalent to the adsorption from the corresponding saturated binary vapor phase. The composition of the binary vapor phase was estimated using the NRTL activity coefficient model [30]. Therefore, using the available pure vapor isotherms of the components of the binary liquid mixtures, we have utilized the rigorous thermodynamic frameworks of the generalized Langmuir isotherm (gL) [24] and the adsorbed solution theory (AST) [25-28] to compute adsorption from the saturated binary vapor phase.

The gL framework provided qualitative correlations for the six binary systems while requiring no computationally expensive spreading pressure calculations of the AST framework. Moreover, it was found that the gL correlations of binary systems involving n-heptane significantly improved after adjusting the molecular area value of n-heptane. It highlights the importance of the availability of accurate experimental data of pure component isotherms. It also suggests that the pure component gL parameters should be regressed by reconciling the pure and binary adsorption isotherm data simultaneously. The binary interaction parameters regressed for the area-based aNRTL adsorbed phase activity coefficient model [24] as implemented in gL are close to zero, indicating nearly ideal adsorbed phase behavior for the six binary systems.

In the AST approach, we have correlated the surface excess using both the ideal adsorbed solution theory (IAST) [25] and the real adsorbed solution theory (RAST) [26-28] coupled with the aNRTL adsorbed phase activity coefficient model [29]. Both the IAST and RAST correlations show a good agreement with the experimental surface excess data [6,18]. It can be inferred from the satisfactory IAST predictions that the adsorbed phase for the six binary liquid mixtures adsorbed on silica gel is nearly ideal, in line with the gL results.

The gL and AST thermodynamic frameworks presented in this work for liquid adsorption do not make any assumptions regarding the adsorbent heterogeneity and the structure of the adsorbed phase, and they should be very useful in simulation, design and implementation of liquid adsorption processes. Our future work will extend these frameworks to the adsorption of multicomponent organic solutes from aqueous solutions.

5. ACKNOWLEDGMENTS

Funding support is provided by the U. S. Department of Energy under the grant DE-EE0007888. The authors gratefully acknowledge the financial support of the Jack Maddox Distinguished Engineering Chair Professorship in Sustainable Energy sponsored by the J.F Maddox Foundation.

AUTHOR CONTRIBUTIONS

Rajasi Shukre: Conceptualization, data curation, formal analysis, methodology, software, validation, visualization, and writing - original draft.

Shikha Bhaiya: Data curation, formal analysis, methodology, and validation.

Usman Hamid: Methodology, formal analysis, and software.

Hla Tun: Methodology and software.

Chau-Chyun Chen: Conceptualization, funding acquisition, investigation, methodology, project administration, resources, software, validation, , and writing - reviewing and editing.

REFERENCES

[1] Oak Ridge National Laboratory. Materials for separation technologies: Energy and emission reduction opportunities, 2005.

[2] JM Prausnitz, RN Lichtenthaler, and EG De Azevedo.*Molecular thermodynamics of fluid-phase equilibria*. Pearson Education, 1998.

[3] C Triantafyllou and R Smith. The design and optimization of dividing wall distillation columns. In *Energy Efficiency in Process Technology*, pages 351–360. Springer, 1993.

[4] MB Rao and S Sircar. Concentration swing adsorption: Novel processes for bulk liquid separations. In *Precision Process Technology*, pages 345–352. Springer, 1993.

[5] J Rouquerol, F Rouquerol, P Llewellyn, G Maurin, and KSW Sing. *Adsorption by powders and porous solids: principles, methodology and applications*. Academic press, 2013.

[6] DP Valenzuela and AL Myers. *Adsorption equilibrium data handbook*. Prentice Hall, 1989.

[7] DH Everett. Thermodynamics of adsorption from solution. part 1.—perfect systems. *Transactions of the Faraday Society*, 60:1803–1813, 1964.

[8] DH Everett. Thermodynamics of adsorption from solution. part 2.—imperfect systems. *Transactions of the Faraday Society*, 61:2478–2495, 1965.

[9] SG Ash, R Bown, and DH Everett. Thermodynamics of adsorption from solution. adsorption by graphon from binary mixtures of benzene, cyclohexane and n-heptane.

Journal of the Chemical Society, Faraday Transactions 1: Physical Chemistry in Condensed Phases, 71:123–133, 1975.

[10] CE Brown, DH Everett, AV Powell, and PE Thorne. Adsorption and structuring phenomena at the solid/liquid interface. *Faraday Discussions of the Chemical Society*, 59:97–108, 1975.

[11] CE Brown, DH Everett, and CJ Morgan. Thermodynamics of adsorption from solution. the systems (benzene+ ethanol)/graphon and (n-heptane+ ethanol)/graphon. *Journal of the Chemical Society, Faraday Transactions 1: Physical Chemistry in Condensed Phases*, 71:883–892, 1975.

[12] G Schay and L Gy Nagy. Critical discussion of the use of adsorption measurements from the liquid phase for surface area estimation. *Journal of Colloid and Interface Science*, 38(2):302–311, 1972.

[13] I Dehany and LG Nagy. Some correlations of the equilibrium thermodynamics of the adsorption of liquid mixtures at solid-liquid interfaces. *Period. Polytech*, 19:485, 1978.

[14] DH Everett. Thermodynamics of adsorption from non-aqueous solutions. In *Progress in Colloid & Polymer Science*, pages 103–117. Springer, 1978.

[15] DH Everett and RT Podoll. Adsorption of near-ideal binary liquid mixtures by graphon. *Journal of Colloid and Interface Science*, 82(1):14–24, 1981.

[16] DH Everett. Thermodynamics of interfacial phenomena. *Pure and Applied Chemistry*, 53(11):2181–2198, 1981.

[17] S Sircar, J Novosad, and AL Myers. Adsorption from liquid mixtures on solids: Thermodynamics of excess properties and their temperature coefficients. *Industrial & Engineering Chemistry Fundamentals*, 11(2):249–254, 1972.

[18] AL Myers and S Sircar. Thermodynamic consistency test for adsorption of liquids and vapors on solids. *The Journal of Physical Chemistry*, 76(23):3412–3415, 1972.

[19] S Sircar and AL Myers. A thermodynamic consistency test for adsorption from binary liquid mixtures on solids. *AIChE Journal*, 17(1):186–190, 1971.

[20] AL Myers and S Sircar. Analogy between adsorption from liquids and adsorption from vapors. *The Journal of Physical Chemistry*, 76(23):3415–3419, 1972.

[21] S Sircar and AL Myers. Statistical thermodynamics of adsorption from liquid mixtures on solids. i. ideal adsorbed phase. *The Journal of Physical Chemistry*, 74(14):2828–2835, 1970.

[22] S Sircar and AL Myers. Prediction of adsorption at liquid-solid interface from adsorption isotherms of pure unsaturated vapors. *AIChE Journal*, 19(1):159–166, 1973.

[23] S Sircar. Thermodynamics of adsorption from binary liquid mixtures on heterogeneous adsorbents. *Journal of the Chemical Society, Faraday Transactions 1: Physical Chemistry in Condensed Phases*, 82(3):831–841, 1986.

[24] U Hamid, P Vyawahare, H Tun, and CC Chen. Generalization of thermodynamic Langmuir isotherm for mixed-gas adsorption equilibria. *AIChE Journal*, page e17663, 2022.

[25] AL Myers and JM Prausnitz. Thermodynamics of mixed-gas adsorption. *AIChE journal*, 11(1):121–127, 1965.

[26] AL Myers. Activity coefficients of mixtures adsorbed on heterogeneous surfaces. *AIChE journal*, 29(4):691–693, 1983.

[27] E Costa, JL Sotelo, G Calleja, and C Marron. Adsorption of binary and ternary hydrocarbon gas mixtures on activated carbon: experimental determination and theoretical prediction of the ternary equilibrium data. *AIChE Journal*, 27(1):5–12, 1981.

[28] O Talu and I Zwiebel. Multicomponent adsorption equilibria of nonideal mixtures. *AIChE journal*, 32(8):1263–1276, 1986.

[29] H Kaur, H Tun, Ml Sees, and CC Chen. Local composition activity coefficient model for mixed-gas adsorption equilibria. *Adsorption*, 25(5):951–964, 2019.

[30] H Renon and JM Prausnitz. Local compositions in thermodynamic excess functions for liquid mixtures. *AIChE journal*, 14(1):135–144, 1968.

[31] JJ Kipling. *Adsorption from Solutions of Non-electrolytes*. Academic Press, 2017.

[32] CK Chang, H Tun, and CC Chen. An activity-based formulation for langmuir adsorption isotherm. *Adsorption*, 26(3):375–386, 2020.

[33] H Tun and CC Chen. Prediction of mixed-gas adsorption equilibria from pure component adsorption isotherms. *AIChE Journal*, 66(7):e16243, 2020.

[34] H Tun and CC Chen. Isosteric heat of adsorption from thermodynamic langmuir isotherm. *Adsorption*, 27(6):979–989, 2021.

[35] I Langmuir. The adsorption of gases on plane surfaces of glass, mica and platinum. *Journal of the American Chemical society*, 40(9):1361–1403, 1918.

[36] HI Britt and RH Luecke. The estimation of parameters in nonlinear, implicit models. *Technometrics*, 15(2):233–247, 1973.

[37] FR Siperstein and AL Myers. Mixed-gas adsorption. *AIChE journal*, 47(5):1141–1159, 2001.

[38] X Cai, F Gharagheizi, LW Bingel, D Shade, KS Walton, and DS Sholl. A collection of more than 900 gas mixture adsorption experiments in porous materials from literature meta-analysis. *Industrial & Engineering Chemistry Research*, 60(1):639–651, 2020.

[39] AL McClellan and HF Harnsberger. Cross-sectional areas of molecules adsorbed on solid surfaces. *Journal of Colloid and Interface Science*, 23(4):577–599, 1967.

[40] TL Hill. Statistical mechanics of multimolecular adsorption. iv. the statistical analog of the bet constant a 1 b 2/b 1 a 2. hindered rotation of a symmetrical diatomic molecule near a surface. *The Journal of Chemical Physics*, 16(3):181–189, 1948.

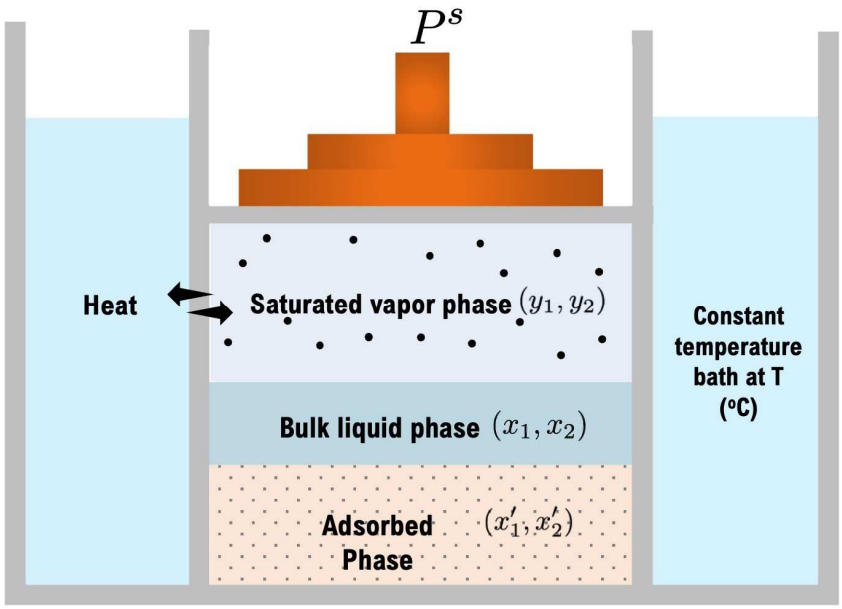

Figure 1: **Equilibrium thermodynamic system for binary liquid mixture adsorption**

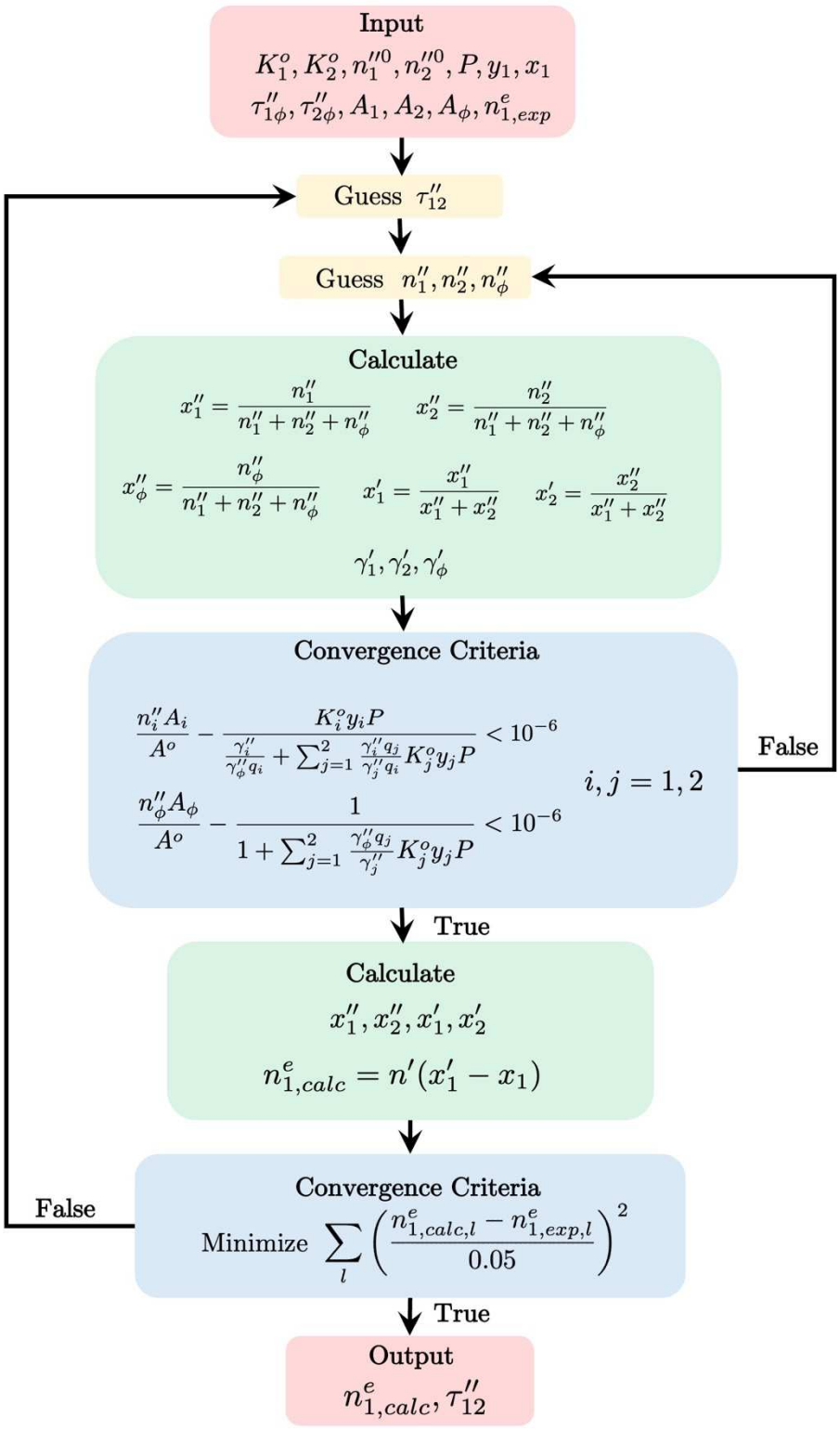

Figure 2: **Algorithm for calculation of adsorption from binary liquid mixtures using the generalized Langmuir isotherm;** Here, *l* stands for the index of data points.

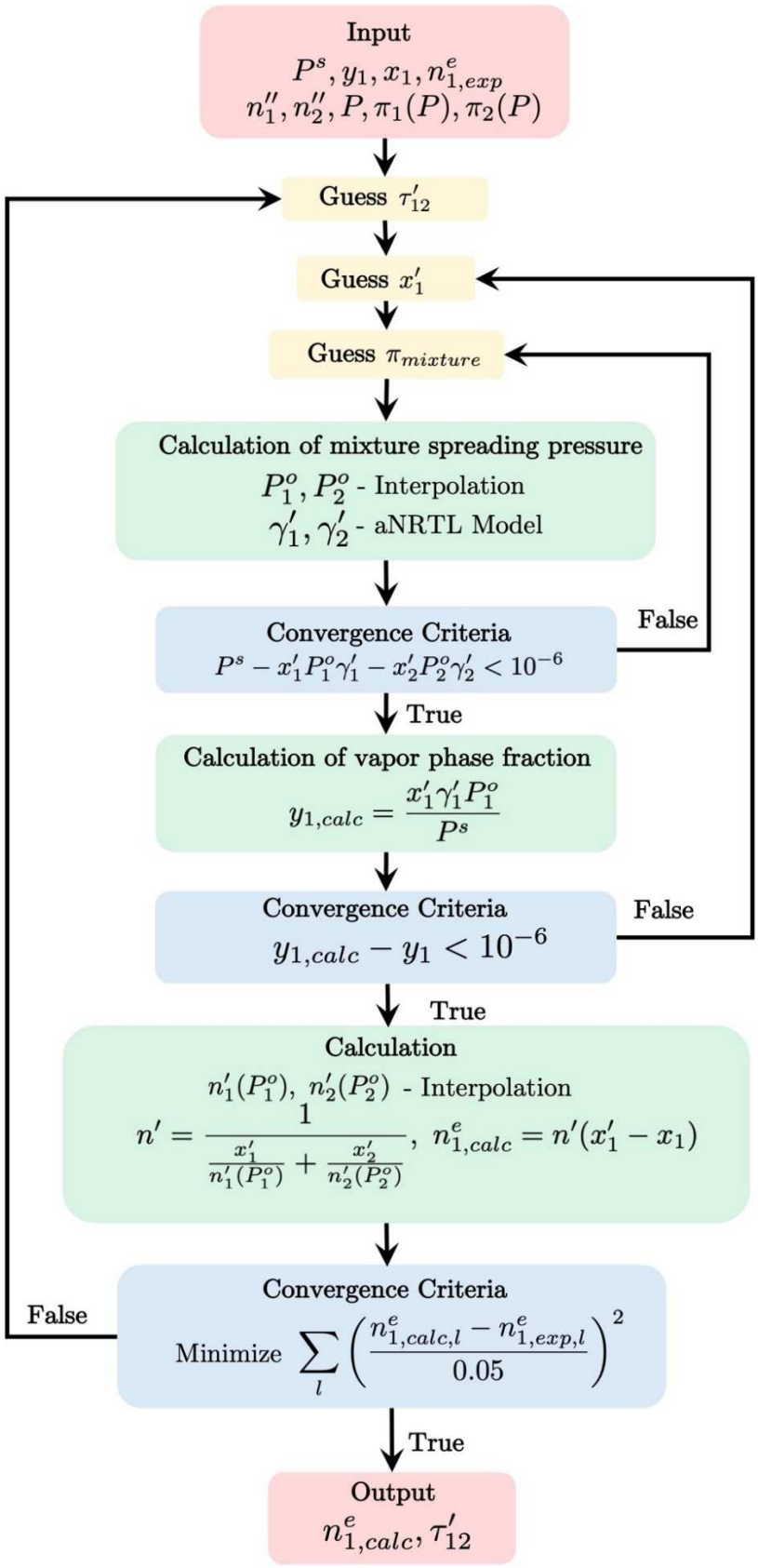

Figure 3: **Algorithm for calculation of adsorption from binary liquid mixtures using the Adsorbed Solution Theory**; *Here, l stands for the index of experimental data points, n''_1 and n''_2 are the amounts adsorbed for pure vapor components 1 and 2 for a given range of pressure (P) calculated using gL isotherm.*

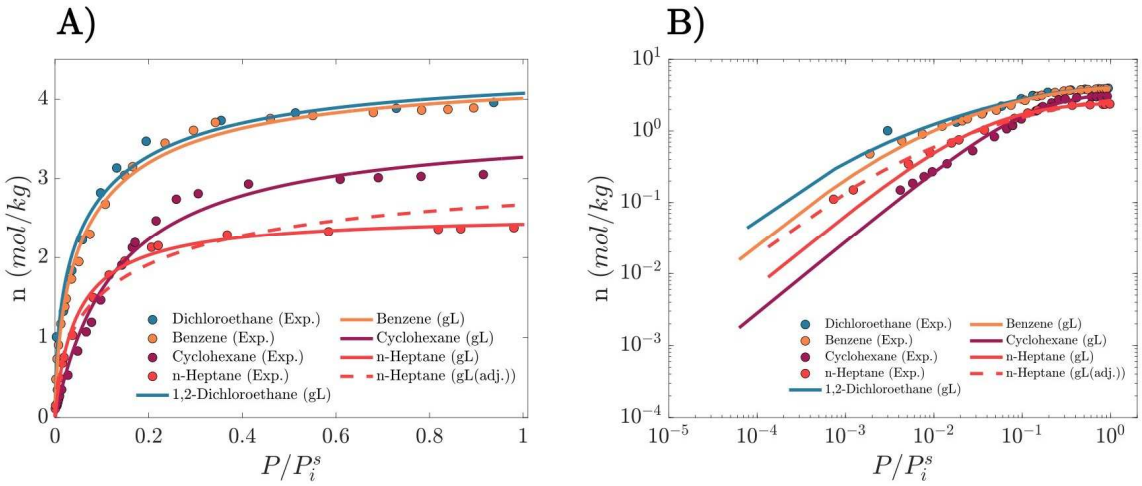

Figure 4: **generalized Langumir correlations of pure component isotherms on silica gel at 303 K A) Linear scale B) Logarithmic scale**. *The experimental (Exp.) data for 1,2-dichloroethane is from ref. [18] and the data for benzene, cyclohexane, and n-heptane is from ref. [6]. P_i^s is the saturation pressure of pure adsorbate tabulated in Table 1, adj. refers to the adjusted area of n-heptane, with gL parameters given in Table 1.*

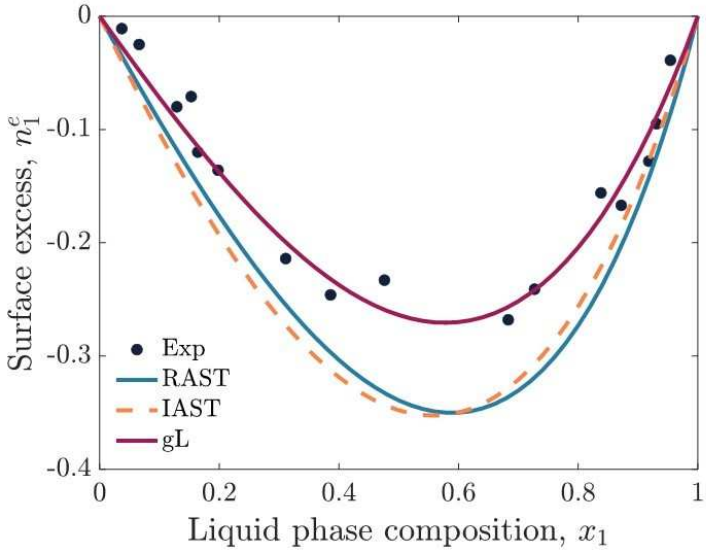

Figure 5: **Surface excess of benzene (1)–1,2-dichloroethane (2) mixture on silica gel at** 303 K; *Experimental data is from [18].*

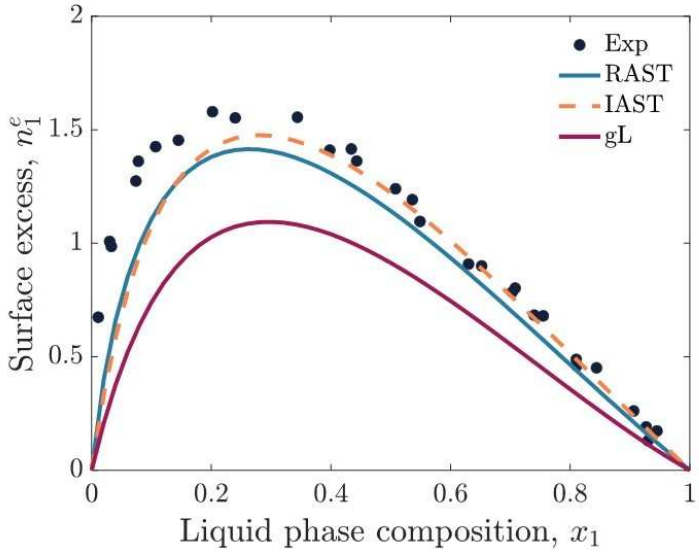

Figure 6: **Surface excess of benzene (1)–cyclohexane (2) mixture on silica gel at 303 K.**; *Experimental data is from [6].*

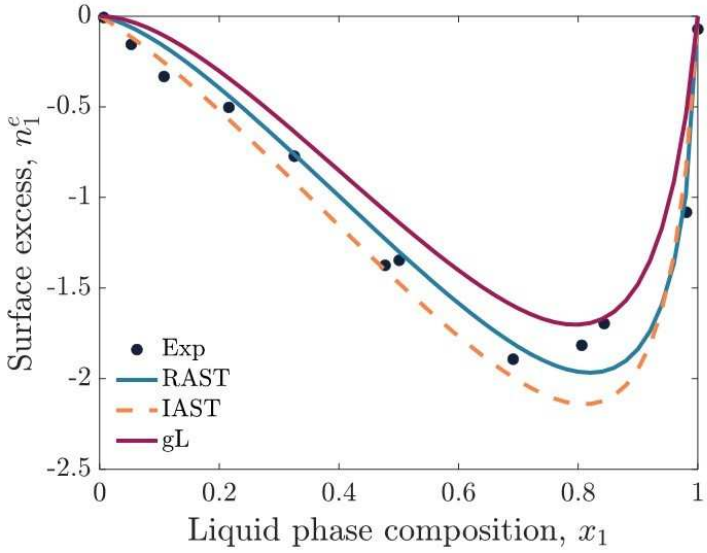

Figure 7: **Surface excess of cyclohexane (1)–1,2-dichloroethane (2) mixture on silica gel** at 303 K.; *Experimental data is from [18].*

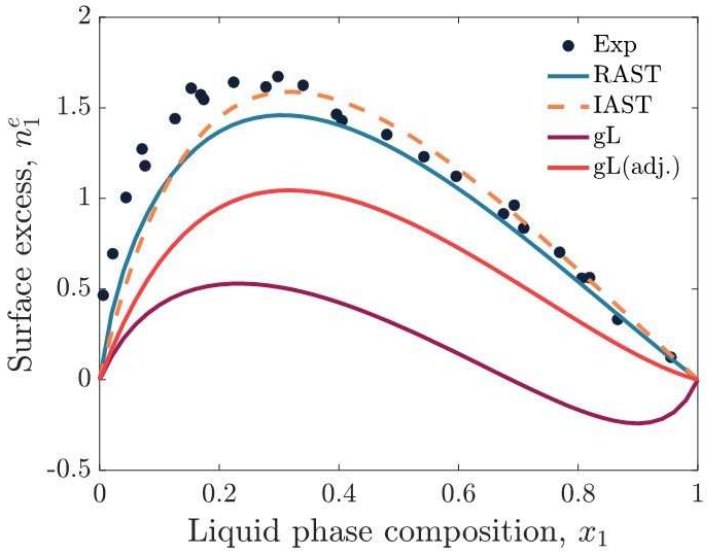

Figure 8: **Surface excess of benzene (1)–n-heptane (2) mixture on silica gel at 303 K.**; *Experimental data is from [6].*

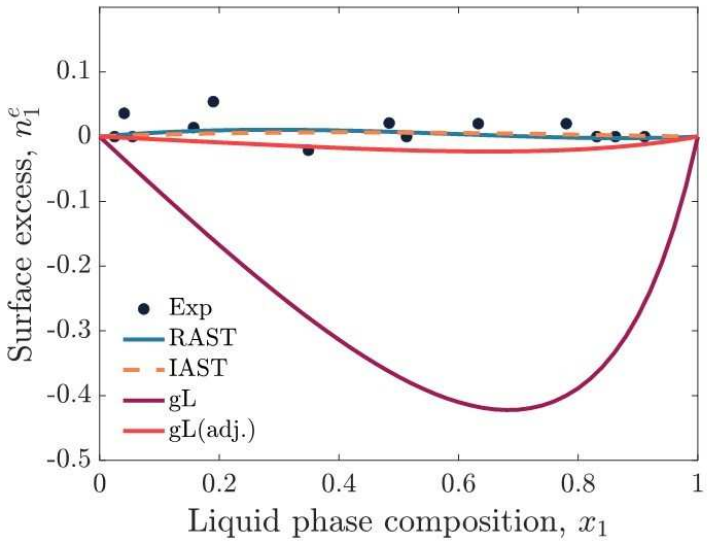

Figure 9: **Surface excess of cyclohexane (1)–n-heptane (2) mixture on silica gel at 303** K.; *Experimental data is from [6].*

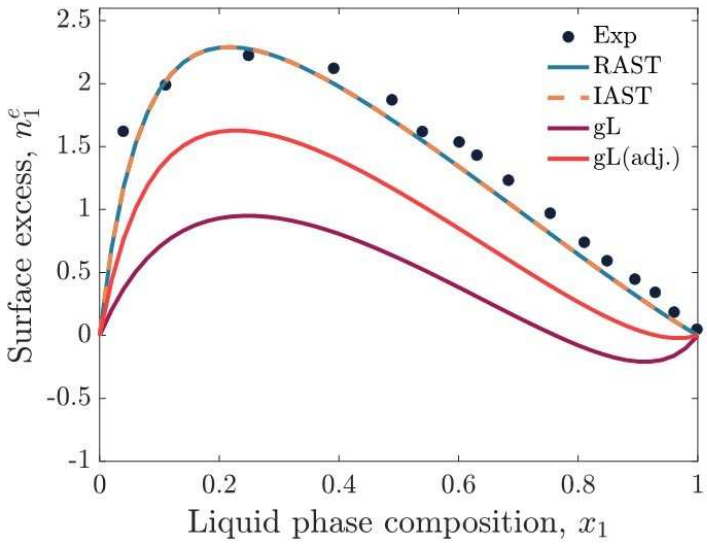

Figure 10: **Surface excess of 1,2-dichloroethane (1)–n-heptane (2) mixture on silica gel at 303 K**; *Experimental data is from [18].*